

Surface Modification of Electroacoustic Device for Underwater pMUT

Roszairi Haron, Mohd Ikhwan Hadi Yaacob, Rosly Jaafar, Muhd Rashidi Abd Razak

¹ Department of Physics, Faculty of Science and Mathematics, Universiti Pendidikan Sultan Idris,
35900 Tanjong Malim, Perak, Malaysia

*Corresponding Author: roszaيري@fsmpt.upsi.edu.my

Abstract: Fabrication routine of piezoelectric micromachined ultrasonic transducer (pMUT) requires complex and repetitive processes which consumes a lot of time and very costly. Deposition of Polydimethylsiloxane (PDMS) as an adhesive layer on silicon substrate has been done using spin coating. The role of this bonding is to adhere the Lead Zirconate Titanate (PZT) wafer. Another layer of PDMS is deposited on top of the PZT to manipulate device's performance and also acting as protection layer. The thickness of the PDMS is controlled by the amount of current applied to D.C. motor. The current used in this study is 1.0 A, 1.2 A and 1.4 A. The performance characteristic of pMUT is done by analysis the electrical properties. High resolution images of surface topography produced by Scanning Electron Microscopy with Energy Dispersive X-ray spectroscopy (SEM/EDX) and Atomic Force Microscopy (AFM) showed that the surface of the PDMS coating was smooth. It is better for wetted/submerged underwater application that require minimum hydrophobic characteristics of the acoustic matching layer. The results clearly proved that this wafer bonding process can simplified the fabrication routine of Piezoelectric Micromachined Ultrasonic Transducer (pMUT) without compromising the performance of the device.

Keywords: pMUT; PDMS; Piezoelectric

1. Introduction

Recent studies showed that piezoelectric Micromachined Ultrasonic Transducers (pMUT) have been extensively developed [1,2,3,4]. However, designing it requires a lot of complex and repetitive processes that include four to five layers of metallic material deposition for electrodes, 20-30 steps of sol-gel of piezo-ceramic film deposition depending on the desired thickness and regular masking, etching, patterning of the substrate for membrane/diaphragm forming. Fabricated pMUTs not only went through various fabrication routine but also lack of resonance frequency and receiving sensitivity.

Conventional fabrication cycle for pMUT requires multiple depositions and etchings of several material layers on the substrate. Alternatively, wafer bonding technique offers simpler fabrication cycle with comparably satisfactory outcome for miniaturize acoustic device [7]. Furthermore, wafer bonding allows pre-manufactured on-the-shelf piezoelectric film and elastic silicon wafers to be adhered using a layer of adhesive to form a functional pMUT device.

This work proposed surface modification approach using polymer material to control open circuit receiving response (OCRR) and transmitting voltage response (TVR) of the pMUTs developed exclusively for immersion applications. We utilize polydimethylsiloxane (PDMS) as an adhesive layer for wafer bonding and coating/protective layer to simplified fabrication routine and at the same time gain control on the device response. The usage of polymeric materials as part of vibrating membrane is widely studied elsewhere [5,6].

2. Materials and Methods

2.1 Polymer Adhesion Layer

Polymer adhesive offers many advantages for permanent wafer adhesion such as high bond strength at lower temperature for practically any substrate materials [8]. As part of the structural composite, polymer adhesion layer will contribute to the overall device performance thus affecting vibration behavior of pMUT structure as depicted in Figure 1.



Figure 1. PMUT fabricated using adhesive wafer bonding of PDMS polymer

2.2 PDMS Protective-Functional Layer

Single-side polished Si wafer was utilized as a substrate for pMUT as the selected design as in Figure 1 does not require membrane or diaphragm structure. Double sided polish Si wafer also employed in several cases for different device architecture [9,10]. The wafer is placed on the ABS casing which was designed using 3D printer previously. It is important to make sure that the wafer is fixed in the casing so that it is not vibrating during rotation especially at high spinning rate.

We have developed a low-cost spin coater for the coating process. The intention of re-inventing spin-coater is made so that the setup can be embedded in an existing STEM syllabus at secondary and tertiary level educations in Malaysia. One of the essential facts of a D.C. motor is that the shaft torque is proportional to the applied current, no matter what the voltage value. There are three samples with selected current produced for this study as shown in the Table 1.

Table 1. Parameters for spin coating

Sample	D.C motor current, I (A)
X	1.0
Y	1.2
Z	1.4

After the Si substrate has been coated, a separate drying step is done to further dry the film without substantially thinning it. This can be advantageous for thick films since long drying times may be necessary to increase the physical stability of the film before handling. The sample is naturally drying at 50 °C for 24 hours.

characterization was performed using Wayne Kerr LCR meter with 1.0 VDC drive and parallel equivalent circuit fitting. Two electrical parameters under observation are impedance, Z and phase, D . Electrical characterization were divided into two spectrums for course and fine pattern.

Impedance and phase shift analyses have been carried out on 5 PZT samples denoted as in Table 2. All electrical

Table 2. Parameter for electrical analyses

Sample	Description
A	Unmodified PZT
B	PDMS Coated PZT using similar to sample X setting
C	PDMS Coated PZT using similar to sample Y setting
D	PDMS Coated PZT using similar to sample Z setting
E	Sample X with PZT adhered on top

Two calibration were carried out namely open circuit sweep and short circuit trim across 20 to 100,000 Hz of the frequency. Initially, we only interested on the frequency

below 20 kHz, however the study also included an analysis between 20 and 100 kHz. For a frequency below 20 kHz, the

increment is every 500 Hz while for course pattern above 20 kHz, the increment was every 10 kHz.

3. Results and Discussion

3.1 Layer Thickness

The FESEM-imaging was conducted to measure the thickness of the samples. From the FESEM images, it was found that Sample X with the lowest applied current (1.0 A) has the thickest coating (Figure 2a). Sample Y with D.C. current of 1.2 A yields a thinner film with the thickness ranging from 176.4 to 179.4 μm .

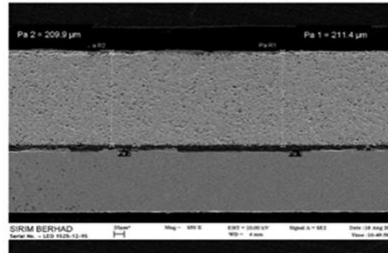


Figure 2(a). Thickness of coating layer of Sample B at 1.0 A spin current and 30 s spin time (209.9-211.4 μm)

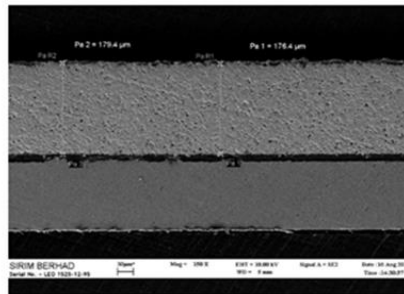


Figure 2(b). Thickness of coating layer of Sample C at 1.2A spin current and 30 s spin time (176.4 - 179.4 μm)

3.2 Effect of PDMS Coating on Impedance

Three samples were analysed and compared namely sample B, C and D. Changes in electrical impedance were

observed between frequency of 10 to 100 kHz as shown in Figure 3(a) while Figure 3(b) shows impedance spectrum between for the frequency ranging from 0.5 – 20 kHz.

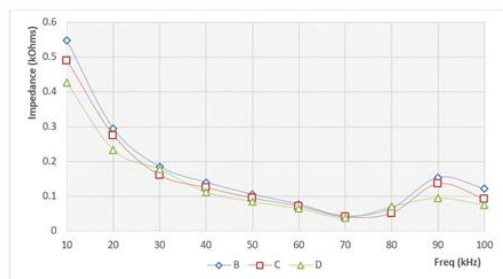


Figure 3(a). Impedance spectrum of coated PZT (10-100 kHz)

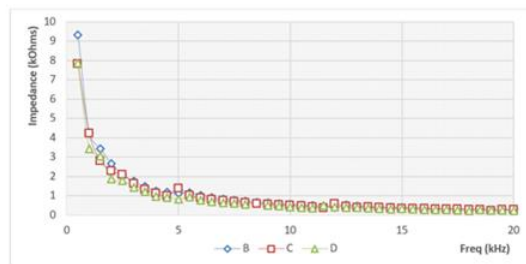


Figure 3(b). Impedance Spectrum of coated PZT (0.5 – 20 kHz)

Based on the findings, Sample B with the thickest PDMS coating yield the highest impedance across the spectrum, followed by Sample C and D, with the thinnest PDMS coating. All three samples show a second harmonic at 90 kHz of frequency and Sample B consistently carry the highest impedance value at the second harmonic.

We can also observe that the PDMS coating on top of the PZT did not alter its bandwidth as seen in Figure 3(a) where all three samples maintain 20 kHz of bandwidth at the second harmonic. However, we only interested on the first harmonic for the targeted underwater applications.

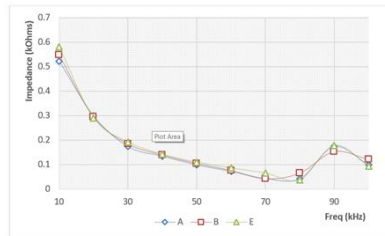


Figure 4(a). Impedance spectrum of PZT (Sample A), coated PZT (Sample B) and Si bonded PZT (Sample E) between 10-100 kHz

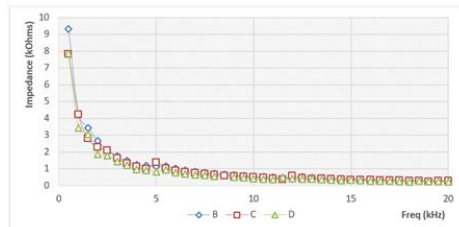


Figure 4(b). Impedance spectrum of PZT (Sample A), coated PZT (Sample B) and Si bonded PZT (Sample E) between 0.5-20 kHz

Interestingly, the anti-resonance of the bonded sample can be clearly observed at approximately 80 kHz, before the impedance value increased dramatically until it reaches a resonance of 90 kHz. When we zoomed in at the spectrum below 20 kHz, similar pattern can be observed and bonded sample has the highest impedance, yielding the best sensitivity across the frequency spectrum. Uncoated sample A was tested as a standard sample for better comparison.

3.3 Effect of PDMS Bonding on Impedance

In this analysis, we investigate and compare the changes in impedance of three PZT samples namely Sample A, B and E. Based on Figure 4(a) and Figure 4(b) we can clearly observe the impedance of Sample E which is a bonded PZT on the Silicon wafer is higher than the other two samples, followed by coated PZT and uncoated PZT has the lowest impedance value. There is no resonance shift can be observed on all samples with similar bandwidth across all samples.

In this investigation, three samples of coated PZT (Sample B, C and D) were studied. Figure 5(a) and Figure 5(b) showed the phase shift on all three samples. The thinnest PDMS coating has resulting in the shift delay during the fourth harmonic. Thick PDMS coating has resulting in the rapid changes in the phase with particularly lower bandwidth.

3.4 Effect of PDMS Coating on Phase

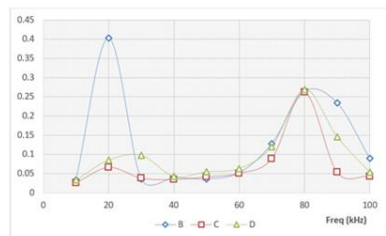


Figure 5(a). Phase shift of three PZT samples coated with PDMS 10-100 kHz

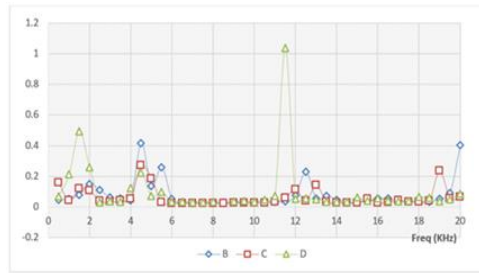


Figure 5(b). Phase shift of three PZT samples coated with PDMS 0.5-20 kHz

The phase shift pattern has become consistent across all samples only on the fifth harmonic at approximately 80 kHz of frequency with thick PDMS sample has resulting in slightly broad bandwidth. More interesting occurrences can be observed below 20 kHz of frequency where 3 resonances occurred as in Figure 5(b). Both analyses revealed that moderately coated PZT (Sample C) has inferior performance compared to heavily coated and lightly coated samples. Other than fourth harmonic, sample B also has the biggest shift during second harmonic. The thinnest coating on the

other hand resulting in the obvious phase shift during first and third harmonics.

3.5 Effect of PDMS Bonding on Phase

Phase shift was significant on the PZT bonded with silicon wafer using PDMS. For the frequency above 20 kHz as illustrated in Figure 6(a), the PZT sample bonded with silicon showed the highest phase shift at the frequency of 90 kHz. For coated PZT sample, phase shift occurs at five different frequencies which are 2 kHz, 4.5 kHz, 12.5 kHz, 20 kHz and 80 kHz approximately.

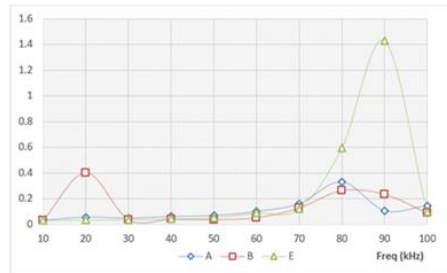


Figure 6(a). Phase shift of uncoated PZT (Sample A), coated PZT (Sample B) and Si bonded PZT (Sample E) between 10-100 kHz

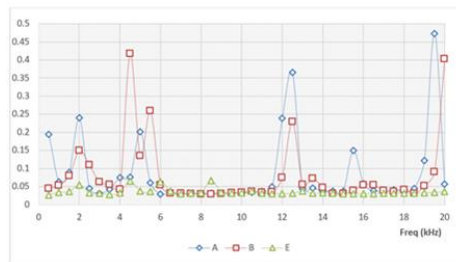


Figure 6(b). Phase shift of uncoated PZT (Sample A), coated PZT (Sample B) and Si bonded PZT (Sample E) between 0.5-20 kHz

For comparison, uncoated PZT has slightly higher occurrences of phase shift that occur 7 times at 500 Hz, 2 kHz, 5 kHz, 12.5 kHz, 15.5 kHz, 20 kHz and 80 kHz. These findings agree with the initial research question that the phase shift can be reduced with thick coating or adhesive coating of the PZT with silicon.

3.6 Coating Material Interaction

Sample D was characterized by scanning electron microscopy (SEM) with energy dispersive X-ray (EDX) analysis (Zeiss LEO 1525). Figure 7(a) shows the image of

the sample area that was scanned. Figure 7(b) and 7(c) revealed the elements detected by the system.

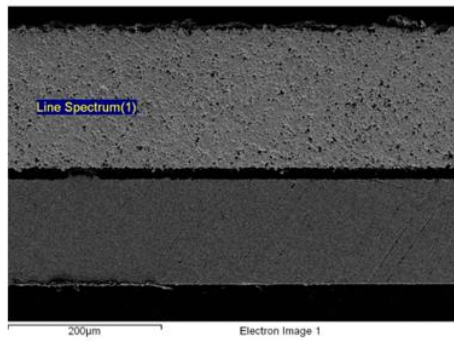


Figure 7(a). PZT layer possible interaction

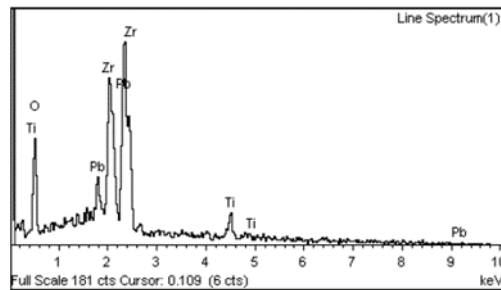


Figure 7(b). No PDMS poisoning detected at PZT layer

Element	Weight%	Atomic%
O K	14.92	58.27
Ti K	6.39	8.34
Zr L	25.17	17.24
Pb M	53.52	16.14
Totals	100.00	

Figure 7(c). PZT composition remain intact after coating process

From Figure 8(a to c), it is clearly shown that there is no other particle exist at the Cu layer. This result is important since the impurities can restrict the process of producing a nice and clean pMUT.

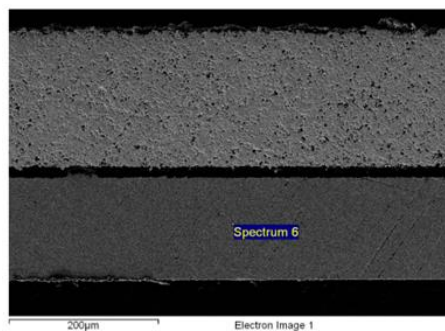


Figure 8(a). No PDMS poisoning detected at Cu layer

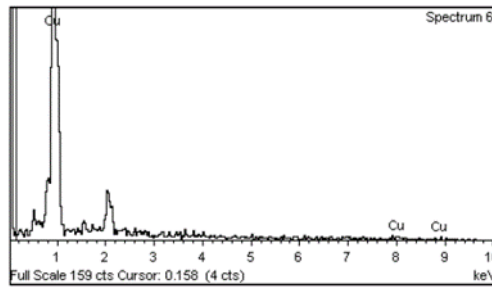


Figure 8(b). Cu layer possible interaction

Element	Weight%	Atomic%
Cu L	100.00	100.00
Totals	100.00	

Figure 8(c). Cu composition remain intact after coating process

3.7 Surface Roughness (AFM)

The surface morphology of the samples were characterized by Atomic Fourier Transform (AFM Bruker Innova). Figure 9(a) shows the 2-D surface morphology of

the sample in Z range of 50.8 nm. Figure 9(b) and 9(c) display 3-D images in Z-range of 10.1 nm and 19.0 nm respectively.

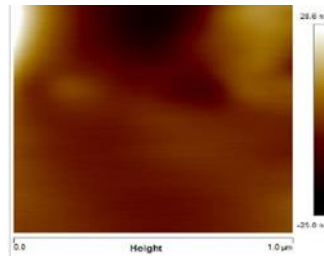


Figure 9(a). Spot 1 (2-D) – Z range of 50.8 nm (1 μm scan spot) and 30.65nm (500 nm scan spot)

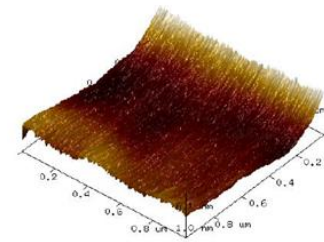


Figure 9(b). Spot 2 (3-D) – Z range of 10.1 nm (1 μm scan spot) & 21.5 nm (500 nm scan spot)

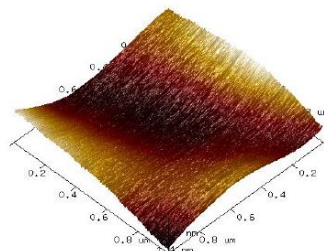


Figure 9(c). Spot 3 (3-D) – Z range of 19.0 nm (1 μm scan spot) & 23.1 nm (500 nm scan spot)

4. Conclusion

The responsivity and sensitivity of the pMUT can be manipulated using top layer coating and adhesive layer bonding. The wafer bonding technique enables us to simply the methods of fabricating pMUT with promising results. However, rapid phase shift should be expected at the higher frequency spectrum region, thus might affected the actual applications for underwater usage.

Spin coating is suitable for PDMS layer thickness control as it produces significant thickness difference with different amount of applied current. It is clearly shown that room temperature wafer bonding has resulting in zero material interaction thus producing clean functional layer for pMUT with the ease of layer deposition. PDMS coating provide exceptional smoothness on the surface for better wetted/submerged underwater application that require minimum hydrophobic characteristics of the acoustic matching layer.

5. Acknowledgement

The authors thank Sultan Idris Education University for providing the research fund (2017-0012-102-01).

References

- [1] Pedersen, T., Zawada, T., Hansen, K., Lou-Moeller, R. & Thomsen, E. (2010). Fabrication of High-Frequency pMUT Arrays on Silicon Substrates. *IEEE Transactions on Ultrasonics, Ferroelectrics, and Frequency Control*, 57, 1470–1477
- [2] Akasheh, F., Myers, T., Fraser, J.D., Bose, S. & Bandyopadhyay, A. (2004) Development of piezoelectric micromachined ultrasonic transducers. *Sensors and Actuators A: Physical*, 111, 275–287
- [3] Sadeghpour, S., Kraft, M., & Puers, R. (2019). Design and fabrication of a piezoelectric micromachined ultrasound transducer (pMUT) array for underwater communication. *2019 International Congress on Ultrasonics*, 38, 1–5
- [4] Li, J., Ren, W., Fan, G. & Wang, C. (2017). Design and Fabrication of Piezoelectric Micromachined Ultrasound Transducer (pMUT) with Partially-Etched ZnO Film. *Sensors 2017*, 17, 1–13
- [5] Wang, Z., Miao, J. & Tan, C. W. (2009). Acoustic Transducers with a perforated damping backplate based on PZT/silicon wafer bonding technique. *Sensors and Actuators A: Physical*, 149, 277–283
- [6] Lam, T. Y., Lam, K. H. & Chan, H. L. W. (2005). Micromachined Piezoelectric Polymer Membrane Acoustic Sensor. *Integrated Ferroelectrics*, 76, 31–37
- [7] Wang, Z., Miao, J. & Tan, C. W. (2009). Acoustic transducers with a perforated damping backplate based on PZT/silicon wafer bonding technique. *Sensors and Actuators A: Physical*, 149, 277–283
- [8] Mohd Ikhwan, H. Y., Mohd Rizal, A., Asrulnizam, A. M. & Mohamad Faizal, A. R. (2011). Vibration Analysis of pMUT with Polymer Adhesion Layer. *RSM2011 Proceeding*, 52–55
- [9] Duval, F. F. C., Dorey, R. A., Wright, R. W., Huang, Z. & Whatmore, R. W. (2004). Fabrication of PZT Composite Thick Films for High Frequency Membrane Resonators. *Journal of Electroceramics*, 13, 267–270
- [10] Polcawich, R. G., Scanlon, M., Pulskamp, J., Clarkson, J., Conrad, J., Washington, D. & Dubey, M. (2003). Design and Fabrication of a Lead Zirconate Titanate (PZT) thin film acoustic sensor. *Integrated Ferroelectrics*. 54, 595–606